

EVALUATING THE EFFECTS OF DISTANCE AND LASER INCIDENCE ANGLES ON
MEASUREMENTS GENERATED BY THE AUTONOMOUSLY OPERATING
TERRESTRIAL LASER SCANNER (ATLS)

A Thesis
Presented in Partial Fulfillment of the Requirements for the
Degree of Master of Science
with a
Major in Natural Resources
in the
College of Graduate Studies
University of Idaho
by
Jessica E. Sanow

Major Professor: Jan Eitel, Ph.D.
Committee Members: Alex Fremier Ph.D.; Lee Vierling, Ph.D.
Department Administrator: Patrick Wilson, Ph.D.

June 2016

AUTHORIZATION TO SUBMIT THESIS

The thesis of Jessica E. Sanow, submitted for the degree of Master of Science with a major in Natural Resources and titled, "EVALUATING THE EFFECTS OF DISTANCE AND LASER INCIDENCE ANGLES ON MEASUREMENTS GENERATED BY THE AUTONOMOUSLY OPERATING TERRESTRIAL LASER SCANNER (ATLS)," has been reviewed in final form. Permission, as indicated by the signatures and dates given below, is now granted to submit final copies to the College of Graduate Studies for approval.

Major Professor: _____ Date: _____
Jan Eitel, Ph.D.

Committee Members: _____ Date: _____
Lee Vierling, Ph.D.

_____ Date: _____
Alex Fremier, Ph.D.

Department
Administrator: _____ Date: _____
Patrick Wilson, Ph.D.

ABSTRACT

Snow depth measurements are critical in ecology, snow water equivalent measurements, and disaster risk assessment. LiDAR based Terrestrial Laser Systems (TLS) have proven capable to generate 3D scans providing information regarding snow depths, these scans typically have low temporal resolution data scans and are high in cost (>\$40,000 USD). The Autonomously Operating Terrestrial Laser Scanner (ATLS) is a unique system that can generate high temporal resolution data scans at a low cost, although, this data has not yet been validated. Scans produced by ATLS were studied to quantify the effects of laser incidence angles and distances to determine the accuracy of the snow depths. The study found that ATLS was capable of generating data with marginally significant effects due to distance and angles ($p = 0.07$). It was found that at distances 10-20 and 30-40 meters from the ATLS results in a snow depth error of 5.98% and 4.03%, respectively.

ACKNOWLEDGEMENTS

I would like to thank Dr. Jan Eitel for choosing me to participate in this study and for all of his help along the way. Dr. Eitel spent countless hours helping to look over my data and edit my writing, there is no way I could have done this without him. Also, I want to thank Dr. Lee Vierling and Dr. Alex Fremier for agreeing to be on my committee and working me into their busy schedules. And lastly, I would like to thank the McCall Outdoor Science School for allowing me to be apart of their spectacular graduate program.

TABLE OF CONTENTS

AUTHORIZATION TO SUBMIT THESIS.....	ii
ABSTRACT.....	iii
ACKNOWLEDGEMENTS.....	iv
TABLE OF CONTENTS.....	v
LIST OF TABLES.....	vii
LIST OF FIGURES.....	viii
1. INTRODUCTION	1
1.1 Effects of Snow Depth on Local Ecology	1
1.2 Effects of Snow Depth on Climate	3
1.3 Effects of Snow Depth on Society.....	4
1.4 SNOTEL	5
1.5 Alternative Snow Depth Measurement Methods.....	7
1.6 ATLS.....	8
1.7 Study Objectives	8
2. METHODS	9
2.1 Control Study	9
2.2 Field Studies	9
2.2.1 Bear Basin Site Description	10
2.2.2 MOSS Site Description	10
2.3 Data Processing.....	11
2.3.1 Control Study.....	11
2.3.2 Bear Basin	12
2.3.3 MOSS	12
2.4 Statistics.....	13
3. RESULTS	16
3.1 Effects of Distance on ATLS Generated Data	16
3.2 Effects of Incidence Angles on ATLS Generated Data	17
3.3 Variability within the SNOTEL Pillow	17
4. DISCUSSION	19
4.1 Effects of Distance on ATLS.....	19
4.2 Effects of Laser Incidence Angles on ATLS.....	20
4.3 Strengths and Limitations of Study	20

5. CONCLUSIONS.....22
WORKS CITED.....23
APPENDIX I.....32
APPENDIX II.....33
APPENDIX III.....39
APPENDIX IV.....41
APPENDIX V.....43

LIST OF TABLES

TABLE 1: FARO AND ATLS SPECIFICATIONS.....	22
TABLE 2: MOSS SITE SNOW DEPTH STAISTICS.....	22

LIST OF FIGURES

FIGURE 1: CONTROL STUDY DIAGRAM.....	23
FIGURE 2: BEAR BASIN SNOTEL SITE.....	24
FIGURE 3: ATLS POINT CLOUD.....	24
FIGURE 4: DIAGRAM OF SNOW STAKES AROUND ATLS, INSET OF ATLS.	25
FIGURE 5: HAND MEASURED VS ATLS SNOW DEPTHS	25
FIGURE 6: HAND VS ATLS DEPTHS GROUPE BY DISTANCE.....	26
FIGURE 7: BOXPLOT OF CONTROL STUDY RESULTS GROUPE BY ANGLE.....	26
FIGURE 8: SNOTEL VS ATLS SNOW DEPTHS (CM).....	27
FIGURE 9: ATLS VS HAND MEASUREMENTS REGRESSION LINES.....	27
FIGURE 10: DIAGRAM OF SHADOWING EFFECT.....	28

1. INTRODUCTION

Snow is the dominant form of precipitation in the northern hemisphere (Artan et al., 2013) and contributes to one-sixth of the world's drinking water supply (Barnett et al., 2005). Detailed measurements of snowpack depth, volume, and density are critical for economic, social and natural systems. Avalanche studies (Datt et al., 2008; Mock and Birkeland, 2000), snow-water equivalent measurements (Grunewald et al., 2010; Jacobson, 2010), earth-atmosphere interactions (Artan et al., 2013; Langlois and Barber, 2008), climate modeling (Brooks et al., 2011; Jones et al., 2000; Luzi et al., 2009), disaster risk assessment (Artan et al., 2013), winter recreation (Grunewald et al., 2010), and ecological studies (Deems et al., 2013; Issak et al., 2010) are just a few examples that require an understanding of the snowpack throughout the winter season. With a warming climate, it is more critical now than ever to have instrumentation to monitor and accurately measure the snowpack (Barnett et al., 2010; Jacobson, 2010)

1.1 Effects of Snow Depth on Local Ecology

Local ecology is greatly dependent on snow depth. Den selection (Chadwick, 2010; Durner et al., 2003; Gaines, 2003; Immell et al., 2013; Magoun & Copeland, 1998), snow insulation (Palacio et al., 2015; Vico et al., 2014), soil temperature (Schimel et al., 2004), mineralization processes (Schimel et al., 2004), vegetation growth (Palacio et al., 2015; Post & Forchhammer, 2008; Vico et al., 2014), and water temperature (Isaak et al., 2010) are just some of the factors reliant on the depth of the snow. Wolverines (*Gulo gulo*) (Chadwick, 2010; Magoun & Copeland, 1998), polar bears (*Ursus maritimus*) (Durner et al., 2003), and black bears (*Ursus americanus*) (Gaines, 2003; Immell et al., 2013) are three species of fauna

that require a substantial snowpack to den during the winter months. Wolverines, for example, only den within snow depths of specifically 2.5-3 meters depth provides enough insulation for warmth, yet is close enough to the surface to attack prey (Chadwick, 2010). Denning occurs during the months February to April, making it essential for the snowpack to last until then (Magoun & Copeland, 1998).

Snowpack provides insulation for several species of shrubs and grasses. This insulation protects the flora from the cold winter temperatures and winds (Palacio et al., 2015). Without the snowpack, these species could be easily killed in the harsh winter temperatures. If the snowpack melts too early, then the plants become susceptible to experiencing springtime freeze-thaw events. Exposure to too many freeze-thaw cycles in a short amount of time can lead to death of the plant (Palacio et al., 2015; Vico et al., 2014)

Soil temperature throughout the winter season is controlled by the depth and duration of the snowpack (Schimel et al., 2004). Soil temperature is directly related to the N mineralization rate during the winter season with N mineralization rates increasing with increasing soil temperatures (Schimel et al., 2004). Many plants are adapted to bloom during peak N mineralization rates, therefore, a snowpack melting early in spring causes an abundance of N mineralization, altering the timing of plant available N for growth (Schimel et al., 2004). The majority of Arctic mammals have timed the production of offspring to match peak vegetation growth (Post & Forchhammer, 2008). Consequently, an early plant growth season can cause a lack of available resources for new offspring (Post & Forchhammer, 2008).

Variation in snow pack depth and duration also affects stream temperatures (Isaak et al., 2010). Isaak et al. (2010), found that smaller snowpacks lead to an increase in stream

temperature by 0.38 C due to the lack of snow cooling the water during melt season. This increase in stream temperature resulted in a 11-20% decrease of spawning Bull trout.

1.2 Effects of Snow Depth on Climate

Snowpack is a key component in both local and global climate systems. Locally, snowpack can affect relative humidity (Barnett et al., 2005), evapotranspiration (Barnett et al., 2005), drought (Barnett et al., 2005; Grunewald et al., 2010), and year-round water availability (Barnett et al., 2005; Grunewald et al., 2010). Early spring runoff causes high erosion rates (Grunewald et al., 2010), an early increase in soil moisture content altering plant and humidity cycles (Barnett et al., 2005), and drought, due to lack of water storage for the late summer when reservoir water is necessary (Barnett et al., 2005; Grunewald et al., 2010). In order to accurately understand and model these local melt systems, the small scale variability (1-10 meters) of the snowpack needs to be taken into account, otherwise prediction models will be greatly over or under estimated (Anderson et al., 2002).

On a global scale, an increase in snowpack depth, distribution, and duration leads to a decrease in air temperature because of snow albedo (Park et al., 2013; Langlois and Barber, 2008; Wang et al., 2015). By definition, snow albedo is the measure of how well a snowpack reflects solar energy; the more snow cover, the less shortwave radiation is absorbed into the ground due to the high reflectance ability of snow (National Snow and Ice Data, n.d.; Sato, 2001). Absorbed shortwave radiation regulates the timing of snow melt, making snow albedo the greatest climate driver in the northern hemisphere (Wang et al., 2015). Grain size and small scale variability is the primary factor that controls the amount of this absorbed shortwave radiation (Wang et al., 2015). It is important to be able to predict and map this

variability across an entire landscape. A decreasing snowpack and increased amounts of shortwave radiation increase the air temperature resulting in negative implications for several species (Durner et al., 2003; Murray et al., 2006; Park et al., 2013). Moose (*Alces alces*), for example, may be showing a decline in the northern United States over the past decade due to this warming trend (Murray et al., 2006). Moose prefer colder climates and experience heat stroke at temperatures between 14-17° C. Also a reduced snowpack and shorter winter, combined with warmer temperatures leads to an increase in pathogens, lethal to moose (McCann et al., 2013; Murray et al., 2006; Street et al., 2015)

1.3 Effects of Snow Depth on Society

Humans rely heavily on snow for drinking water supply (Grunewald et al., 2010), food availability (Jacobson, 2010), power supply (Barnett et al., 2005; Grunewald et al., 2010), disaster risk assessment (Artan et al., 2013; Datt et al., 2008; Mock and Birkeland, 2000), and winter recreation (Grunewald et al., 2010). A population map from 2000 determined that one-sixth of the human population depends on glaciers and seasonal snowpack for water supply and is reliant on reservoir storage (Barnett et al., 2005). This water storage determines the availability of drinking water supply, crop irrigation, water supply for agriculture, and timing of water release for salmon runs (Barnett et al., 2005). Many statistical models have been created to predict the amount of melt water available following the winter season. However, these models typically over estimate the amount of water since they do not account for the variability in the snow pack (Grunewald et al., 2010). These overestimations of melt water greatly impact all of the previously mentioned factors. Snowpack also insulates crops during the winter from extreme cold weather and provides moisture during the melting season

(Jacobson, 2010). Within the western United States 22% of electricity comes from hydropower. Hydropower is a clean and inexpensive energy producer but is dependent on the availability of snowpack melt water (West, n.d.). Winter tourism and recreation is an important industry in the western United States. In 2009/2010 winter season winter recreation generated 212,000 jobs and provided an economic value of \$12.2 billion (EcoWest, 2013). This industry relies entirely on snow cover duration, depth and reliability (Grunewald et al., 2010).

1.4 SNOTEL

Currently, the western United States and western Canada have established SNOTEL (Snow Telemetry) sites as an in-field method of acquiring daily snow depth measurements (Perkins et al., 2009). The measurements are acquired daily by the use of radio wave burst technology, which is the process of transmitting collected data to the main station by bouncing radio waves off the meteor region in our atmosphere 50 miles above the ground (Scafer & Paetzold, 2000). There are 858 SNOTEL sites within 11 states, and each site costs between \$25,000-35,000 USD initially, and another \$3,000 annually (NRCS, (n.d.); Domonkos et al., (n.d.)). Sites typically consist of a pressure sensitive snow pillow, sonic sensor, thermometer, and precipitation storage gauge (National Water & Climate Center, 2016). The pressure exerted on the snow pillow by the weight of the snow calculates the mass of the snow. The thermometer on the SNOTEL site is shielded to measure air temperature, and the precipitation storage gauge captures and stores cumulative precipitation throughout the winter season (National Water & Climate Center, 2016). The sonic sensor is mounted directly above the snow pillow to take snow depth measurements based on the speed

of the return of the sonic pulse (NRCS, n.d.).

Although SNOTEL sites can accurately measure snow depth, they are limited by a single point of snow depth measurement with a beam-width of 22° and an accuracy of +/- 2 inches (NRCS & USDA, 2010). Because of this single point measurement, SNOTEL does not sufficiently represent the variability within snowpack (Dressler et al., 2006; Molotch & Bales, 2005). Boulders (Lopez et al., 2011; Lopez-Moreno et al., 2011), branches (Lopez et al., 2011), vegetation (Lopez et al., 2011; Lopez-Moreno et al., 2011; Jost et al., 2007), streams (Lopez-Moreno et al., 2011), micro-topography (Jost et al., 2007), crystalline structure (Jost et al., 2007), wind redistribution (Erikson et al., 2005; Jost et al., 2007), canopy cover (Jost et al., 2007; Lopez et al., 2011; Watson et al., 2006), elevation (Erikson et al., 2005; Jost et al., 2007), aspect (Jost et al., 2007), sublimation (Jost et al., 2007), shortwave and long wave radiation (Jost et al., 2007) all influence the snowpack. Thus a single point depth measurement is incapable of representing the variability of the snowpack throughout a watershed (Lopez et al., 2011; Molotch & Bales, 2005).

Small scale variability is caused by branches, boulders, vegetation contained within a small plot of the snowpack (Lopez et al., 2011; Lopez-Moreno et al., 2011). Lopez et al., (2011) found that within a 10x10 meter plot the mean depth varied between 73-134 centimeters in January and 65-253 centimeters in April. Lopez and colleagues concluded that in order to accurately portray a snowpack at least 5 snow depth measurements must be taken at a 2-meter spacing for a 10x10 meter plot for an error to be <10%, and 8 measurements for an error to be 5%. Therefore, a greater amount of snow depth measurements leads to a more accurate snow pack representation (Lopez et al., 2011).

Large scale snow depth variability is caused by various types of elevation, aspect,

canopy cover and ground cover within a single watershed (Jost et al., 2007; Watson et al., 2006). Jost et al. (2007) found that these factors contributed to 80-90% variability of snow accumulation within a watershed. Watson et al. (2006) found that various ground and canopy covered landscapes (i.e. burned forests, meadows, etc.) resulted in up to a 61% variation within the snowpack. Wind, topography, and vegetation variation cause variability from 1 meter to 100 meter scales, which can lead to very inaccurate results if it is not taken into account (Deems et al., 2006).

SNOTEL sites using a single-point measurement over an entire watershed have been found to consistently over-predict the amount of snowpack within a watershed (Molotch & Bales, 2005). This overestimation is because SNOTEL does not take the large scale or small scale variability in snow depth into account (Dressler et al., 2006; Molotch & Bales, 2005). An overestimation of the snowpack could have serious consequences when designing a water budget during a drought year (Dressler et al., 2006). A 2% error for a single-point SNOTEL measurement translated over an entire 100 square-meter watershed is equivalent to a loss or gain of 2 centimeters of water (Dressler et al., 2006).

1.5 Alternative Snow Depth Measurement Methods

In contrast to SNOTEL's single point measurement, Terrestrial Laser Scanners (TLS) are capable of surveying areas of the snowpack ranging from 100 to 800 meters (Prokop et al., 2008). These scans consist of hundreds of thousands of data points with spacing up to 30 mm while operating in varied environments (Prokop, 2008). However, limiting factors within the TLS system still exist, such as a high cost (>\$40,000 USD) and in order to obtain high temporal resolution, TLS scans are time and labor intensive (Eitel et al., 2013). These high

resolution scans require many repeated scans over large areas; this also involves the set-up of targets to tie TLS surveys together (Eitel et al., 2013).

1.6 ATLS

The recent availability of Autonomously Operating Terrestrial Laser Scanners (ATLS) could be a time and cost-effective method for snow depth measurements. ATLS is a unique system with the ability to generate highly spatially and temporally resolved data scans at a relatively low cost (<12,000 USD) (Eitel et al., 2013). The ATLS is capable of generating hundreds of thousands of snow depth readings within its field of view on a daily basis while operating autonomously.

Previous studies, such as Eitel et al. in 2013, tested the ATLS under several weather conditions and found that the ATLS was capable of running without any interruptions. ATLS has also been found capable of closely monitoring snow depths and detecting avalanches on site (Adams et al., 2013). Additionally, LeWinter and colleagues have used the ATLS for year-long monitoring of remote outlet glaciers in Alaska and Greenland (LeWinter et al., 2014). However, the accuracy of ATLS derived snow depth measurements has not been validated.

1.7 Study Objectives

It was the overarching goal of this research to assess the accuracy of the ATLS derived snow depth estimates. The specific objectives were to test how ATLS measurements were affected by the 1) distance between the laser and the surface and 2) the angle of incidence.

2. METHODS

To answer the two objectives, three different experiments were established, one experiment under controlled laboratory conditions (hereafter referred to as the control experiment) and two field experiments (hereafter referred to as Bear Basin and MOSS).

2.1 Control Study

The control study consisted of approximately 130 Ping-Pong balls cut in half and attached to a 1x1 meter board. ATLS was set up 25 meters away from the board, which was set at an angle of 0° perpendicular to ATLS and a scan was taken, shown in Figure 1. The board was then adjusted to 45° and 66° angles with an ATLS scan being taken at each angle, also shown in Figure 1. The Ping-Pong board was then moved to 50, 75, and 150 meters from the ATLS, and the process was repeated for each angle at each distance. For accuracy comparison, a scan by the FARO Focus3D X 330 (FARO, (n.d.)) as a comparison standard, the specifications for both the FARO and ATLS are shown in Table 1 (FARO, (n.d.); Eitel et al., 2013).

2.2 Field Studies

Two sites were chosen for the study over the course of two separate winter seasons - Bear Basin in 2012-2013 and the McCall Outdoor Science School (MOSS) Field Campus in 2014-2015. Bear Basin is located 8.5 kilometers north of McCall, Idaho, in Adams County at 44°55'34.47" N, 116°5'16.08" W. The second site, McCall Outdoor Science School Field Campus (MOSS), is located 2.4 kilometers away from McCall, Idaho in Valley County at

44°59'38.21" N, 116°7'31.99" W. The study sites are approximately 8 kilometers in distance from each other with a difference in 98 meters of elevation.

2.2.1 Bear Basin Site Description

Bear Basin is at an elevation of 1,630 meters and is a year round popular outdoor recreation area. The study site was located on SNOTEL site number 319, named Bear Basin (Figure 2), which has been recording data since July 13, 1980 (NRCS, 2015). Blue spruce (*Picea pungens*) and Douglas fir (*Pseudotsuga menziesii*) are the predominant tree species in the study area. The average annual precipitation at the Bear Basin site is 45-64 centimeters and the average annual air temperature is 2-5°C (Soil Survey Staff, 2015).

The ATLS was mounted to the SNOTEL tower, and measurements of the surrounding objects (i.e. trees, poles, fences) within a scan radius of around 30 meter were recorded (Figure 3). The ATLS scans were taken between November 11, 2012 and May 7, 2013 within the same field of view as the SNOTEL. To determine the accuracy of ATLS's data, the snow depths measured by the ATLS were compared to corresponding snow depth readings, provided by the SNOTEL's sonar sensor.

2.2.2 MOSS Site Description

The McCall Outdoor Science School is at an elevation of 1,532 meters and is located on the McCall Field Campus of the University of Idaho, College of Natural Resources. The Ponderosa Pine (*Pinus ponderosa*) is the main species in the field site. The average annual precipitation is 58-68 centimeters and the average annual air temperature is 3-5°C (Soil Survey Staff, 2015).

ATLS was placed in a clearing of trees with sixteen snow stakes set up radially around the stand. Figure 4 is a diagram of the snow stakes set up in groups of four, placed at 10, 20, 30 and 40 meters from ATLS. The ATLS scans were taken from December 17, 2014 to April 7, 2015 and the scan radius was approximately 75 meters.

Snow depth measurements made by ATLS were compared to hand measurements taken at every snow stake during periods of significant snowfall or melting (e.g. rain on snow) events.

2.3 Data Processing

For each of the three study sites, the data scans were loaded into Cloud Compare (Cloud Compare (Version 2.6.2), n.d.) to view the ATLS derived scan as a 3D point cloud, a detailed description of the process found in Appendix III. The 3D point cloud was examined to ensure all necessary data existed and then were loaded into MATLAB (MATLAB, 1990). All depth calculations were performed using MATLAB, as well as the statistical analysis. A detailed description of the process is found in Appendix IV for the MOSS site and Appendix V for the control study.

2.3.1 Control Study

ATLS scans were loaded into MATLAB and reduced to only include the Ping-Pong covered board. Next, a simulated board was generated to match the length and width dimensions of the original board (1x1 meters); the depth was limited to exclude the Ping-Pong balls. The two boards were converted into two separate mesh grids by using the MATLAB function meshgrid. Following this, the simulated board was subtracted from the board with the Ping-Pong balls. The leftover value was the volume of the Ping-Pong balls on the board.

The difference between the true volume and the MATLAB generated volume represents the error caused by distance and/or angle. A detailed outline of this exact process and codes is found in Appendix IV. This true volume was obtained by a FARO scan, a 3D laser scanner (FARO, (n.d.)). The FARO scan was loaded into MATLAB and underwent the same process to determine the volume.

2.3.2 Bear Basin

The Bear Basin site was used to compare ATLS generated snow depths to SNOTEL produced snow depths. ATLS scans were loaded into Cloud Compare and three random points were chosen from the point cloud. Two ATLS generated scans were loaded into MATLAB, a snow-covered scan and a snow-free scan. Both scans were converted into mesh grids and the snow-free scan was subtracted from the snow-covered scan, the leftover number was the depth of the snow in centimeters. This process was done for each of the three randomly selected points. At each point the depth was calculated for a 20 cm² area and a 100 cm² area. SNOTEL depths were retrieved from the NRCS website for the corresponding ATLS scan dates.

2.3.3 MOSS

Using Cloud Compare, the 16 snow stakes were located in the point cloud and the XY coordinate was recorded. Next, a snow-free scan and snow-covered scan were loaded into MATLAB and each scan was converted into two separate mesh grids. The snow-free scan was then subtracted from the snow-covered scan, leaving the snow depth at each snow stake.

Hand depths were taken at each of the snow stakes and compared to the corresponding ATLS derived snow depths.

2.4 Statistics

To answer the first study objective, the effect of distance on ATLS measurements, a linear regression was performed. The following assumptions were checked to carry out the linear regression:

1. Linear relationship
2. Multivariate normality
3. No or little multi-collinearity
4. No auto-correlation
5. Homoscedasticity

The first linear regression model was used to determine if the ATLS generated snow depths and the hand measured snow depths were statistically significant compared to each other from the MOSS field study. The model was fit to the following equation:

$$\text{ATLS snow depth} = \text{Slope} * \text{Hand measured snow depth} + \text{error}$$

Within this model coefficient of determination (r^2), root mean squared deviation (RMSD) (Pineiro et al., 2008), slope, intercept, p-value, and average differences were calculated. The coefficient of determination describes the relationship between the actual and predicted values, a r^2 of 0 indicates no correlation and a r^2 of 1 indicates high correlation. The RMSD represents the mean deviation of predicted values with respect to the observed one (Pineiro et

al., 2008). Lower RMSD values indicate high precision. Slope and intercept describe the line that fits the modeled regression data. The p-value represents the probability of a study to show the same results within a confidence interval, $p < 0.05$ indicate to reject the null and $p > 0.05$ indicate to fail to reject the null. The null in this case is that the distances found by ATLS and hand measurements are equal within a 95% confidence bound.

The second model used the difference of the ATLS generated snow depths and the hand measured depths and distance as a covariate and determined if there was a statistically significant difference between the of the tested distances (10, 20, 30, and 40m). The coefficient of determination (r^2), root mean squared deviation (RMSD) (Pineiro et al., 2008), slope, intercept, p-value, and average differences were computed for the second regression model as well.

To answer the second study objective, the effect of the angle of incidence on ATLS measurements, a two-factor ANOVA with no repetition model was performed. The following assumptions were checked before carrying out the two-way ANOVA:

1. Normal distribution
2. Independent
3. Variances must be equal
4. Same sample size

Hypotheses:

$$H_0: \text{Angle}_0 = \text{Angle}_{45} = \text{Angle}_{66}$$

$$H_0: \text{Distance}_{25} = \text{Distance}_{50} = \text{Distance}_{75} = \text{Distance}_{150}$$

$$H_a: \text{At least one angle or distance is not equal}$$

The model had two factors, angles and distances. It used the differences between ATLS scans and the FARO scan to determine if the difference between the two volumes was significant by calculating the p-value and average differences.

The last statistical analysis was a simple linear regression model run on the Bear Basin site, the same assumptions were checked as objective 1. The Bear Basin site was used to represent the variability in snow depth measurements within the SNOTEL snow pillow area. All three ATLS points from around the snow pillow were used as the x, or predictor, variables and the SNOTEL depths were used as the y, or response variables. The coefficient of determination (r^2), root mean squared deviation (RMSD), slope, intercept, p-values, and average differences were computed.

3. RESULTS

3.1 Effects of Distance on ATLS Generated Data

The first linear regression model, comparing ATLS generated snow depth and hand measured snow depths, found a strong correlation with an r^2 value of 0.73 and an RMSD value of 10.44 cm. These values indicate that between the hand measured values and the ATLS generated snow depths there is a strong, positive relationship, thus verifying ATLS derived snow depths have an accuracy within +/- 10.44 cm. Although this error seems small, applied over an entire landscape could lead to an extreme under or over estimation of the snowpack (Dressler et al., 2006; Molotch & Bales, 2005). If this error is applied over a 100 m² area of a watershed, this could mean that 10.44 cubic meters (2,758 gallons) of water is unaccounted. Figure 5 shows the hand measured snow depths versus the ATLS generated snow depths within a 95% confidence bound plotted with the linear fit model from the regression as well as the 1:1 line.

It was this discovery that led to the second linear regression models, using each distance (10, 20, 30, and 40 meters) as a covariate, the results shown in Table 2. Figure 6 is a scatter plot of the results, the data is grouped by distance and plotted with a 1:1 line and the regression line. This regression led to an interesting finding that the highest RMSD value of each of the four distances was the 10-meter distance at 6.55 cm and the lowest was the 30-meter distance with an RMSD of 2.56. As discussed previously, these errors seem small until applied over an entire watershed, an error at 10 meters results to a 6.55 m³ (1,730 gallons) of excess or lost water. Although 30 meters had the lowest, therefore most accurate RMSD, it had the only p-value lower than the 0.05 threshold. This indicates that the values within the 30-meter range reject the null stating that the values may differ within a 95% confidence

interval. It also can indicate that the sample size was too small to make any definite conclusions.

The two-factor ANOVA for the control study produced a p-value for the four distances used during the control experiment. The calculated p-value was 0.55 at a 99% confidence interval, $\alpha = 0.01$. These results indicated that the difference between the ATLS and FARO scans is not statistically significant due to distance.

3.2 Effects of Incidence Angles on ATLS Generated Data

The two-factor ANOVA found that no tested angle (0, 45, and 66°) produced a measurement error that was statistically significant within a 99% confidence interval, $\alpha = 0.01$. The p-value between the three groups of angles was 0.07, which does indicate there is some evidence that there a marginal effect, but there is not enough data within the groups to make a definite conclusion. Other studies, such as one done by Kukko et al. (2008), found similar results that incidence angle has little to no impact on the overall quality of the scan. Figure 7 is a boxplot showing the results of the ANOVA grouped by angles.

3.3 Variability within the SNOTEL Pillow

The overall r^2 value for SNOTEL generated snow depth and ATLS generated snow depths was 0.98, indicating a strong, positive correlation between the snow depths. The RMSD value was 9.71 cm and a p-value < 0.05 , rejecting the null and accepting the alternative hypothesis that at least one of the values between the two snow depths is statistically significant within a 95% confidence interval, $\alpha = 0.05$. The slope was 1.00 (+/- 0.01) and the y-intercept -3.89 (+/- 0.78). Figure 6 shows SNOTEL snow depths vs. ATLS

snow depths plotted with the linear fit line and confidence bounds and Figure 7 is a histogram of the residuals. These results help to prove the importance of multiple data points to correctly interpret snow depths (Dressler et al., 2006; Molotch & Bales, 2005). Figure 8 shows the ATLS and SNOTEL depths plotted by Julian Date in 2012.

4. DISCUSSION

4.1 Effects of Distance on ATLS

The regression model using a distance covariate showed that the 30-meter distance had an unusually low p-value compared to the other three distances indicating a potential error. When this inconsistency was further explored it was found that the 30-meter distance the least amount of data points of any of the four distances. The ATLS was able to pick the area near the snow stake, but not enough for the interpolation and subtraction process like the other areas. Plants and shrubs were also noted as a potential cause of error because they blocked the direct line of site in some cases. It is likely that the lack of points at the 30-meter distance is what caused this low p-value, which is typical in most 3D TLS scanning systems (Prokop, 2008).

The snow stakes at the 30 and 40 meter distances were sometimes difficult to locate in the 3D point scan in Cloud Compare. This is expected since trees, shrubs and other vegetation are the likely in the area and can be the cause of the inability to locate the snow stakes at the farther distances. Eitel and colleagues, (2013), found similar results when using ATLS to map tree canopies and estimated diameter at breast height (DBH) of trees. They found that ATLS could provide reliable scan data of the canopy 20-26 meters away. From the previous experiments, as well as the results from here, potentially, the best use for ATLS could be within similar ranges of 15-26 meters.

Another interesting discovery from the regression with a distance covariate revealed that the RMSD value for the 10-meter distance was 6.55 cm, the highest out of all other RMSD values. This discrepancy is also noticed in Figure 9, which shows the regression lines grouped by each distance and the 1:1 line. The plot shows the regression lines for the 10 and

20-meter distance having a higher slope than the 30 and 40-meter distances. This overestimation could be attributed to laser infiltration of the snowpack at close distances.

4.2 Effects of Laser Incidence Angles on ATLS

Although the study found that angles had no significant effect on the ATLS scans, some errors are still noticed based on the shadowing effect caused by trees, shrubs, rocks, etc., in higher distance scans. An example of the shadowing effect is shown in Figure 10. It is caused by long distance scans resulting in low angle incidence angles causing the microtopography in the snowpack to create long shadows resulting in lack of data points behind the objects. The shadowing effect can create an underestimation of snow depth, which can be noticed in Figure 9. This phenomenon does the exact opposite of scans at closer distances, which can cause laser infiltration, but is able to obtain more points around objects.

4.3 Strengths and Limitations of Study

Sample size seemed to be the major limitation of this study, especially with the control study. Only one scan was taken per distance and angle making comparisons and statistical analysis very challenging. It was this reason that the differences between the FARO and ATLS scans were used as opposed to a direct comparison of ATLS and FARO at each angle and distance. The MOSS field study also had limited data. ATLS scan days and hand measurements were typically one day off from each other, and so only four days aligned and were used. Out of these four days, two had extremely high humidity or snow which is another potential issue with TLS systems ((Adams et al., 2013; Deems et al., 2013; Eitel et al., 2013). Lack of a direct line of sight is a notable potential error as mentioned when discussing the 30-

meter distance at the MOSS site. Adams and colleagues (2013) used ATLS to scan a mountainside over a winter season and also found that without direct line of sight or poor conditions the ATLS scans were unreliable. As previously discussed, laser infiltration and the shadowing effect also create the potential for error in the snow depths.

From the study it was determined that clear targets and fair (low humidity) weather seem to provide more accurate results, although ATLS is still capable of running and producing satisfactory results during fog, high humidity, rain, and snow events. Large targets with a direct line of sight are easily identified in 3D point scans up to 150 meters away, which was discovered during the control study. Small (1-inch diameter) snow stakes, although not easy, can be identified up to 40 meters from the ATLS. The data is also user-friendly, meaning it is easily load into a variety of programs, such as MATLAB and Cloud Compare.

Since the study showed that angles and distances have only a marginal effect on accuracy, ATLS could be reliable for a variety of uses such as canopy cover, crop height, avalanche studies, and snow depths. Similar studies to this one with larger sample sizes could greatly benefit the future of ATLS. Comparisons of ATLS scans during various types of weather would also be a beneficial study in order to account for weather as an error.

5. CONCLUSIONS

The purpose of this study was to examine ATLS derived data to determine if scans were affected by incidence angles and distance to determine if ATLS is capable of producing high quality, accurate snow depths. To complete the validation, the specific objectives are to test how ATLS snow depth measurements are affected by the 1) distance between the laser and the surface and 2) angle of incidence Overall, the study found that the ATLS was capable of generating data with only a marginally significant effect due to distance and angles ($p = 0.07$). However, RMSD values found from the study were rather high, depending on the potential use for the ATLS. The RMSD values ranged from 2.56 to 6.55 cm and these errors could drastically alter results of the study. It was found that distances 10-20 meters from the ATLS can result in a snow depth error of 5.98% and distances 30-40 meters results in an error of 4.03%. These errors seem small, but when applied over an entire 100 m² watershed can result in a 10.44 m³ (2,757 gallons) over or underestimation of water. Several external factors could be the cause of these errors and future studies are needed to fully explore these issues.

It was also found that ATLS and SNOTEL derived snow depths were strongly correlated, however, the difference in the SNOTEL single-point measurement and the ATLS generated snow depths is statistically significant. This is evidence showing that single point measurement SNOTEL is unable to capture the variability within the snowpack, even on the smooth surface of the snow pillow, thus being an unreliable way to predict snow depth. ATLS, on the other hand, is able to capture the variability of the snowpack.

WORKS CITED

- Adams, M.S., Gleirscher, E., Gigele, T., Fromm, R., 2013. Automated Terrestrial Laser Scanner measurements of small-scale snow avalanches, in: International Snow Science Workshop Grenoble – Chamonix Mont-Blanc - 2013. pp. 1060–1065.
- Allee, J. G. (1975). *Webster's dictionary*. New York: Galahad Books.
- Anderton, S., White, S., & Alvera, B. (2002). Micro-scale spatial variability and the timing of snow melt runoff in a high mountain catchment. *Journal of Hydrology*, 268(1-4), 158-176. Retrieved March 30, 2016.
- Artan, G. A., Verdin, J. P., & Lietzow, R. (2013). Large scale snow water equivalent status monitoring: comparison of different snow water products in the upper Colorado Basin. *Hydrology and Earth System Sciences*, 17(12), 5127–5139. <http://doi.org/10.5194/hess-17-5127-2013>
- Assumptions of Linear Regression - Statistics Solutions. (n.d.). Retrieved March 27, 2016, from <http://www.statisticssolutions.com/assumptions-of-linear-regression/>
- Baltsavias, E. (1999). Airborne laser scanning: basic relations and formulas. *ISPRS Journal of Photogrammetry & Remote Sensing*, (54), 199–214. Retrieved from http://www2.geog.ucl.ac.uk/~mdisney/teaching/teachingNEW/PPRS/papers/Baltsavias_Lidar.pdf
- Baker, M., & Ffolliott, P. (2003). Role of Snow Hydrology in Watershed Management. *Journal of the Arizona-Nevada Academy of Sciences*, 35(1), 42-47. Retrieved October 28, 2015, from http://www.fs.fed.us/rm/boise/AWAE/labs/awae_flagstaff/publications/baker_ffolliott_roleofsnowhydrology.pdf
- Barnett, T. P., Adam, J. C., & Lettenmaier, D. P. (2005). Potential impacts of a warming climate on water availability in snow-dominated regions. *Nature*, 438(7066), 303–309. <http://doi.org/10.1038/nature04141>
- Beniston, M. (2003). Climatic change in mountain regions: A review of possible impacts. *Climatic Change*, 59(1-2), 5–31. <http://doi.org/10.1023/A:1024458411589>
- Bokhorst, S., Metcalfe, D. B., & Wardle, D. A. (2013). Reduction in snow depth negatively affects decomposers but impact on decomposition rates is substrate dependent. *Soil Biology and Biochemistry*, 62, 157-164. Retrieved March 1, 2016.
- Brooks P.D., Grogan P., Templer P.H., Groffman P. O., & Schimel J (2011) Carbon and nitrogen cycling in snow-covered environments. *Geogr. Compass*, 5(9), 682–699 (doi: 10.1111/j. 1749-8198.2011.00420.x)

Chadwick, D. H. (2010). *The wolverine way*. Ventura, CA: Patagonia Books.

CloudCompare (Version 2.6.2) [Computer software]. (n.d.). Retrieved May 17, 2015, from <http://www.danielgm.net/cc/>

Datt, P., Srivastava, P. K., Negi, P. S., & Satyawali, P. K. (2008). Surface energy balance of seasonal snow cover for snow-melt estimation in N-W Himalaya. *Journal of Earth System Science*, *117*(5), 567–573. <http://doi.org/10.1007/s12040-008-0053-7>

Deems, J. S., Fassnacht, S. R., & Elder, K. J. (2006). Fractal Distribution of Snow Depth from Lidar Data. *J. Hydrometeor Journal of Hydrometeorology*, *7*(2), 285-297. Retrieved February 27, 2016.

Deems, J. S., Painter, T. H., & Finnegan, D. C. (2013). Lidar measurement of snow depth: A review. *Journal of Glaciology*, *59*(215), 467–479. doi:10.3189/2013JoG12J154

Deems, J.S., Gadowski, P.J., Vellone, D., Evanczyk, R., LeWinter, A., Birkeland, K.W., Finnegan, D.C., (2015). Mapping starting zone snow depth with a ground-based lidar to assist avalanche control and forecasting. *Cold Reg. Sci. Technol.*, in press

Domonkos, B., Landers, L., & Wetlaufer, K. (n.d.). Snowpack Monitoring for Water Supply Forecasting and Drought Planning. Retrieved May 15, 2016, from http://wwa.colorado.edu/events/workshops/docs/2015snowCO/Domonkos_CO_Snow_Workshop_Sep2015.pdf

Durner, G. M., Amstrup, S. C., & Fischbach, A. S. (2003). Habitat characteristics of polar bear terrestrial maternal den sites in northern Alaska. *Arctic*, *56*(1). Retrieved March 14, 2016.

Egli, L., Jonas, T., Grünwald, T., Schirmer, M., & Burlando, P. (2012). Dynamics of snow ablation in a small Alpine catchment observed by repeated terrestrial laser scans. *Hydrological Processes*, *26*(November 2011), 1574–1585. doi:10.1002/hyp.8244

Eitel, J. U. H., Vierling, L. A., & Magney, T. S. (2013). A lightweight, low cost autonomously operating terrestrial laser scanner for quantifying and monitoring ecosystem structural dynamics. *Agricultural and Forest Meteorology*, *180*, 86–96. doi:10.1016/j.agrformet.2013.05.012

FARO. (n.d.). Retrieved March 27, 2016, from <http://www.faro.com/en-us/home>

Gaines, William L. 2003. Black Bear, *Ursus americanus*, denning chronology and den site selection in the northeastern Cascades of Washington. *Canadian Field-Naturalist* *117*(4) 626-633.

Girardeau-Montaut, D., & Roux, M. (2005). Change detection on points cloud data acquired with a ground laser scanner. *International Archives of Photogrammetry, Remote Sensing and*

Spatial Information Sciences, 36, W19. Retrieved from http://www.danielgm.net/phd/isprs_laserscanning_2005_dgm.pdf

Griffith, A. B., & Loik, M. E. (2010). Effects of climate and snow depth on *Bromus tectorum* population dynamics at high elevation. *Oecologia*, 164(3), 821-832. Retrieved March 14, 2016.

Grünewald, T., Schirmer, M., Mott, R., & Lehning, M. (2010). Spatial and temporal variability of snow depth and SWE in a small mountain catchment. *The Cryosphere Discussions*, 4(1), 1–30. <http://doi.org/10.5194/tcd-4-1-2010>

Gutmann, E., 2010. Continuous alpine snow depth mapping by laser rangefinder through a winter season. In: AGU Fall Meeting Abstracts 2010.

Gutmann, E., Larson, K.M., Williams, M.W., Nievinski, F.G., Zavorotny, V., 2011. Snow measurement by GPS interferometric reflectometry: an evaluation at Niwot Ridge, Colorado. *Hydrol. Process.*, 8329, <http://dx.doi.org/10.1002/hy>.

Heilig, A. (2008). Next level for snow pack monitoring in real-time using Ground-Penetrating Radar (GPR) technology. *International Snow*, 111–117. Retrieved from [http://avalancheinf.powweb.com/Canadian Avalanche Association - Industry/ISSW2008Proceedings/Papers/P__8042.pdf](http://avalancheinf.powweb.com/Canadian_Avalanche_Association_-_Industry/ISSW2008Proceedings/Papers/P__8042.pdf)

Helfricht, K., Kuhn, M., Keuschnig, M., & Heilig, A. (2014). Lidar snow cover studies on glaciers in the Alps (Austria): Comparison with snow depths calculated from GPR measurements. *Cryosphere*, 8, 41–57. <http://doi.org/10.5194/tc-8-41-2014>

Hodgson, Michael E., & Patrick Bresnahan. "Accuracy of airborne lidar-derived elevation." *Photogrammetric Engineering & Remote Sensing* 3 (2004): 331-39. Web. 15 Oct. 2015. <http://asprs.org/a/publications/pers/2004journal/march/2004_mar_331-339.pdf>.

Immell, D., Jackson, D. H., & Boulay, M. C. (2013). Denning ecology of American black bears in the Cascade Mountains of western Oregon. *Ursus*, 24(1), 1-12. Retrieved March 14, 2016.

Isaak, D. J., Luce, C. H., Rieman, B. E., Nagel, D. E., Peterson, E. E., Horan, D. L. Chandler, G. L. (2010). Effects of climate change and wildfire on stream temperatures and salmonid thermal habitat in a mountain river network. *Ecological Applications*, 20(5), 1350–1371. <http://doi.org/10.1890/09-0822.1>

Jaakkola, A., Hyypä, J., & Puttonen, E. (2014). Measurement of snow depth using a low-cost mobile laser scanner. *IEEE Geoscience and Remote Sensing Letters*, 11(3), 587–591.

Jacobson, M. D. (2010). Inferring snow water equivalent for a snow-covered ground reflector using GPS multipath signals. *Remote Sensing*, 2(10), 2426–2441. <http://doi.org/10.3390/rs2102426>

Jacobson, M. D. (2014). Estimating snow water equivalent for a slightly tilted snow-covered prairie grass field by GPS interferometric reflectometry. *EURASIP Journal on Advances in Signal Processing*, 2014(1), 61. <http://doi.org/10.1186/1687-6180-2014-61>

Jones H.G., Pomeroy, J.W., Walker, D.A., & Hoham, R.W. (2001) Snow ecology: an interdisciplinary examination of snow- covered ecosystems. Cambridge University Press, Cambridge

Kaasalainen, S., Kaartinen, H., Kukko, A., 2008. Snow cover change detection with laser scanning range and brightness measurements. EARSeL eProceedings 133–141.

Keller, F., & Kienast, F.(2000). Evidence of response of vegetation to climatic change on high elevation sites in the Alps, Switzerland. *Change*, 1(2), 70–77.

Kilian, J., Haala, N., & Englich, M. (1993). Capture and evaluation of airborne laser scanner data 2 AIRBORNE LASER SENSOR. *Scanning*.

Kukko, A., Kaasalainen, S., & Litkey, P. (2008). Effect of incidence angle on laser scanner intensity and surface data. *Appl. Opt. Applied Optics*, 47(7), 986.

Langlois, a., & Barber, D. G. (2008). Advances in seasonal snow water equivalent (SWE) retrieval using in situ passive microwave measurements over first-year sea ice. *International Journal of Remote Sensing*, 29(16), 4781–4802. <http://doi.org/10.1080/01431160801908145>

LeWinter, A. L., et al.. "Can we estimate precipitation rate during snowfall using a scanning terrestrial LiDAR?." AGU Fall Meeting Abstracts. Vol. 1. 2012.

LeWinter, A. L., D. C. Finnegan, G. S. Hamilton, L. A. Stearns, and P. J. Gadowski. "Continuous Monitoring of Greenland Outlet Glaciers Using an Autonomous Terrestrial LiDAR Scanning System: Design, Development and Testing at Helheim Glacier." AGU Fall Meeting Abstracts, Vol. 1, 2014.

Liston, G. E., & Hiemstra, C. A. (2011). Representing grass- and shrub-snow-atmosphere interactions in climate system models. *Journal of Climate*, 24(8), 2061–2079. <http://doi.org/10.1175/2010JCLI4028.1>

López-Moreno, J. I., & Nogués-Bravo, D. (2006). Interpolating local snow depth data: An evaluation of methods. *Hydrological Processes*, 20(May 2005), 2217–2232. <http://doi.org/10.1002/hyp.6199>

Lopez-Moreno, J. I., Fassnacht, S. R., Beguera, S., & Latron, J. B. P. (2011). Variability of snow depth at the plot scale: Implications for mean depth estimation and sampling strategies. *Cryosphere*, 5(3), 617–629. <http://doi.org/10.5194/tc-5-617-2011>

Lopez-Moreno, J. I., Fassnacht, S. R., Heath, J. T., Musselman, K. N., Revuelto, J., Latron, J., ... Jonas, T. (2013). Small scale spatial variability of snow density and depth over complex alpine terrain: Implications for estimating snow water equivalent. *Advances in Water Resources*, 55, 40–52. <http://doi.org/10.1016/j.advwatres.2012.08.010>

Luus, K. A., Gel, Y., Lin, J. C., Kelly, R. E. J., & Duguay, C. R. (2013). Pan-Arctic linkages between snow accumulation and growing-season air temperature, soil moisture and vegetation. *Biogeosciences*, 10(11), 7575–7597. <http://doi.org/10.5194/bg-10-7575-2013>

Luzi, G., Noferini, L., Mecatti, D., Macaluso, G., Pieraccini, M., Atzeni, C., Nagler, T. (2009). Using a ground-based SAR interferometer and a terrestrial laser scanner to monitor a snow-covered slope: Results from an experimental data collection in Tyrol (Austria). *IEEE Transactions on Geoscience and Remote Sensing*, 47(2), 382–393. doi:10.1109/TGRS.2008.2009994

MacDonald, M. K., Pomeroy, J. W., & Pietroniro, A. (2010). On the importance of sublimation to an alpine snow mass balance in the Canadian Rocky Mountains. *Hydrology and Earth System Sciences*, 14(7), 1401–1415. <http://doi.org/10.5194/hess-14-1401-2010>

Magoun, A. J., & Copeland, J. P. (1998). Characteristics of wolverine reproductive den sites. *The Journal of Wildlife Management*, 62(4), 1313. Retrieved March 14, 2016.

Marty, C. (2008). Regime shift of snow days in Switzerland. *Geophysical Research Letters*, 35(12), n/a–n/a. <http://doi.org/10.1029/2008GL033998>

MATLAB. Version. R2015a. South Natick, MA: MathWorks, 1990. Computer software.

McCann, N., Moen, R., & Harris, T. (2013). Warm-season heat stress in moose (*Alces alces*). *Can. J. Zool. Canadian Journal of Zoology*, 91(12), 893-898. Retrieved March 14, 2016.

Mock, C. J., & Birkeland, K. W. (2000). Snow Avalanche Climatology of the Western United States Mountain Ranges. *Bulletin of the American Meteorological Society*, 81(10), 2367–2392. [http://doi.org/10.1175/1520-0477\(2000\)081<2367:SACOTW>2.3.CO;2](http://doi.org/10.1175/1520-0477(2000)081<2367:SACOTW>2.3.CO;2)

Murray, D. L., Cox, E. W., Ballard, W. B., Whitlaw, H. A., Lenarz, M. S., Custer, T. W., Fuller, T. K. (2006). Pathogens, nutritional deficiency, and climate influences on a declining moose population. *Wildlife Monographs*, 166, 1-30. Retrieved March 14, 2016.

National Water & Climate Center, NRCS, & USDA. (2016, February 9). SNOTEL and snow survey & water supply forecasting. Retrieved January 1, 2014, from http://www.wcc.nrcs.usda.gov/snotel/SNOTEL_brochure.pdf

National Geographic. Avalanche Facts, Avalanche Information, Avalanche Videos, Avalanche Photos - National Geographic. (n.d.). Retrieved November 4, 2015, from <http://environment.nationalgeographic.com/environment/natural-disasters/avalanche-profile/>

National Snow and Ice Data Center. (n.d.). Retrieved November 5, 2015, from <https://nsidc.org/cryosphere/seoice/processes/albedo.html>

Natural Resources Conservation Service (NRCS). (n.d.). Bear Basin (319) - Site Information and Reports. Retrieved March 22, 2015, from <http://www.wcc.nrcs.usda.gov/nwcc/site?sitenum=319>

Natural Resources Conservation Service (NRCS). (n.d.). Retrieved November 4, 2015, from http://www.nrcs.usda.gov/wps/portal/nrcs/detail/or/snow/?cid=nrcs142p2_046155

Neumann, N. N., Derksen, C., Smith, C., & Goodison, B. (2006). Characterizing local scale snow cover using point measurements during the winter season. *Atmosphere-Ocean*, 44(3), 257-269. <http://doi.org/10.3137/ao.440304>

NRCS, & USDA. (July 2010). Chapter 2: Data Parameters. *Part 622 Snow Survey and Water Supply Forecasting National Engineering Handbook*, 36. Retrieved February 26, 2016.

NRCS National Water and Climate Center - Publications - Snow Surveys and Water Supply Forecasting (Agriculture Information Bulletin 536) - Snow Surveys - SNOTEL. (n.d.). Retrieved February 25, 2016, from http://www.wcc.nrcs.usda.gov/factpub/sect_4b.html

Özdoğan, M. (2011). Climate change impacts on snow water availability in the euphrates-tigris basin. *Hydrology and Earth System Sciences*, 15(9), 2789–2803. <http://doi.org/10.5194/hess-15-2789-2011>

Painter, T.H., Berisford, D.F., Boardman, J.W., Bormann, K.J., Deems, J.S., Gehrke, F., Hedrick, A., Marks, D., Mattmann, C., McGurk, B., Ramirez, P., Richardson, M., Skiles, S.M., Winstral, A., 2015. The Airborne Snow Observatory: fusion of imaging spectrometer and scanning LiDAR for snow albedo and snow water equivalent. *Remote Sens. Environ.*

Palacio, S., Lenz, A., Wipf, S., Hoch, G., & Rixen, C. (2015). Bud freezing resistance in alpine shrubs across snow depth gradients. *Environmental and Experimental Botany*, 118, 95-101.

Park, H., Walsh, J. E., Kim, Y., Nakai, T., & Ohata, T. (2013). The role of declining Arctic sea ice in recent decreasing terrestrial Arctic snow depths. *Polar Science*, 7(2), 174-187. Retrieved March 14, 2016.

Perkins, T. R., Pagano, T. C., & Garen, D. C. (2009). Innovative operational seasonal water supply forecasting technologies. *Journal of Soil and Water Conservation*, 64(1). Retrieved February 25, 2016, from http://www.wcc.nrcs.usda.gov/ftpref/downloads/factpub/wsf/Perkins_Pagano_Garen_JSWC_2009.pdf

Pineiro, G., S. Perelmea, J.P. Guerschman, and J.M. Paruelo. 2008. How to evaluate models: observed vs. predicted or predicted vs. observed? *Ecological Modelling* 216:316-322.

Pfeifer, N., Höfle, B., Briese, C., Rutzinger, M., & Haring, A. (2008). Analysis of the backscattered energy in terrestrial laser scanning data. *Int. Archives of Photogrammetry, Remote Sensing And Spatial Information Sci.*, 37(2006), 1045–1052.

Pomeroy, J. W., Toth, B., Granger, R. J., Hedstrom, N. R., & Essery, R. L. H. (2003). Variation in Surface Energetics during Snowmelt in a Subarctic Mountain Catchment. *Journal of Hydrometeorology*, 4(4), 702–719. [http://doi.org/10.1175/1525-7541\(2003\)004<0702:VISED>2.0.CO;2](http://doi.org/10.1175/1525-7541(2003)004<0702:VISED>2.0.CO;2)

Post, E., & Forchhammer, M. C. (2008). Climate change reduces reproductive success of an Arctic herbivore through trophic mismatch. *Philosophical Transactions of the Royal Society B: Biological Sciences*, 363(1501), 2367-2373. Retrieved March 14, 2016.

Pollyea, R. M., & Fairley, J. P. (2012). Experimental evaluation of terrestrial LiDAR-based surface roughness estimates. *Geosphere*, 8(1), 222-228. doi:10.1130/ges00733.1

Prokop, A. (2008). Assessing the applicability of terrestrial laser scanning for spatial snow depth measurements. *Cold Regions Science and Technology*, 54(3), 155–163. doi:10.1016/j.coldregions.2008.07.002

Prokop, A., Schirmer, M., Rub, M., Lehning, M., & Stocker, M. (2008). A comparison of measurement methods: Terrestrial laser scanning, tachymetry and snow probing for the determination of the spatial snow-depth distribution on slopes. *Annals of Glaciology*, 49, 210-216. doi:10.3189/172756408787814726

The R Project for Statistical Computing. (n.d.). Retrieved May 17, 2015, from <http://www.r-project.org/>

Sato, T. (2001). Spatial and temporal variations of frozen ground and snow cover in the eastern part of the Tibetan Plateau. *Journal of the Meteorological Society of Japan*. <http://doi.org/10.2151/jmsj.79.519>

Schimel, J. P., Bilbrough, C., & Welker, J. M. (2004). Increased snow depth affects microbial activity and nitrogen mineralization in two Arctic tundra communities. *Soil Biology and Biochemistry*, 36(2), 217-227.

Schöber, J., Achleitner, S., Kirnbauer, R., Schöberl, F., & Schönlaub, H. (2010). Hydrological modelling of glacierized catchments focusing on the validation of simulated snow patterns – applications within the flood forecasting system of the Tyrolean river Inn. *Advances in Geosciences*, 27, 99–109. <http://doi.org/10.5194/adgeo-27-99-2010>

Scafer, G. L., & Paetzold, R. F. (March 2000). SNOTEL (SNOWpack TELemetry) And SCAN (Soil Climate Analysis Network). *Automated Weather Stations for Applications in*

Agriculture and Water Resources Management: Current Use and Future Perspectives. Retrieved February 25, 2016, from <ftp://meteor.wcc.nrcs.usda.gov/downloads/factpub/soils/SNOTEL-SCAN.pdf>.

Schöner, W., Auer, I., & Böhm, R. (2009). Long term trend of snow depth at Sonnblick (Austrian Alps) and its relation to climate change [Abstract]. *Process. Hydrological Processes*, 23(7), 1052-1063. Retrieved March 14, 2016.

Singh, K. K., Datt, P., Sharma, V., Ganju, a., Mishra, V. D., Parashar, a., & Chauhan, R. (2011). Snow depth and snow layer interface estimation using Ground Penetrating Radar. *Current Science*, 100(10), 1532–1539.

Soil Survey Staff, Natural Resources Conservation Service, United States Department of Agriculture. Web Soil Survey. Available online at <http://websoilsurvey.nrcs.usda.gov/>. November 16, 2015

Snow jobs: America's \$12 billion winter sports economy and climate change - EcoWest. (2013, December 3). Retrieved November 5, 2015, from <http://ecowest.org/2013/12/03/snow-jobs/>
Snow Telemetry (SNOTEL) and Snow Course Data and Products. (n.d.). Retrieved November 4, 2015, from <http://www.wcc.nrcs.usda.gov/snow/>

Stirling, I., & Derocher, A. E. (2012). Effects of climate warming on polar bears: A review of the evidence. *Global Change Biology*, 18(9), 2694-2706. Retrieved March 14, 2016.

Street, G. M., Rodgers, A. R., & Fryxell, J. M. (2015). Mid-day temperature variation influences seasonal habitat selection by moose. *Jour. Wild. Mgmt. The Journal of Wildlife Management*, 79(3), 505-512. Retrieved March 14, 2016.

Tinkham, W. T., Smith, A. M. S., Marshall, H. P., Link, T. E., Falkowski, M. J., & Winstral, A. H. (2014). Quantifying spatial distribution of snow depth errors from LiDAR using Random Forest. *Remote Sensing of Environment*, 141, 105–115.
doi:10.1016/j.rse.2013.10.021

Trujillo, E., Ramírez, J. A., & Elder, K. J. (2007). Topographic, meteorologic, and canopy controls on the scaling characteristics of the spatial distribution of snow depth fields. *Water Resources Research*, 43(7), W07409. <http://doi.org/10.1029/2006WR005317>

Vico, G., Hurry, V., & Weih, M. (2014). Snowed in for survival: Quantifying the risk of winter damage to overwintering field crops in northern temperate latitudes. *Agricultural and Forest Meteorology*, 197, 65-75.

Vihma, T., Mattila, O.-P., Pirazzini, R., & Johansson, M. M. (2010). Spatial and temporal variability in summer snow pack in the Dronning Maud Land, Antarctica. *The Cryosphere Discussions*, 4, 1107–1150. <http://doi.org/10.5194/tcd-4-1107-2010>

Vroom, G. W., Herrero, S., & Ogilvie, R. T. (1980). The ecology of winter den sites of grizzly bears in Banff National Park, Alberta. *Bears: Their Biology and Management*, 4, 321. Retrieved March 14, 2016.

Walsh, N., McCabe, T., Welker, J., & Parsons, A. (1997). Experimental manipulations of snow-depth: Effects on nutrient content of caribou forage. *Global Change Biology*, 3(S1), 158-164.

Wang, T., Peng, S., Krinner, G., Ryder, J., Li, Y., & Dantec, S. (2015). Impacts of Satellite-Based Snow Albedo Assimilation on Offline and Coupled Land Surface Model Simulations, 2, 1–19. <http://doi.org/10.1371/journal.pone.0137275>

West | National Hydropower Association. (n.d.). Retrieved November 3, 2015, from <http://www.hydro.org/why-hydro/available/hydro-in-the-states/west/>

Weather History for KMYL - February, 2015. (n.d.). Retrieved March 01, 2016, from https://www.wunderground.com/history/airport/KMYL/2015/2/20/DailyHistory.html?req_cit y=&req_state=&req_statename=&reqdb.zip=&reqdb.magic=&reqdb.wmo=&MR=1

Wipf, S., Stoeckli, V., & Bebi, P. (2009). Winter climate change in alpine tundra: Plant responses to changes in snow depth and snowmelt timing. *Climatic Change*, 94(1-2), 105-121. Retrieved March 14, 2016.

Zhong, X., Zhang, T., & Wang, K. (2014). Snow density climatology across the former USSR. *The Cryosphere*, 8(2), 785–799. <http://doi.org/10.5194/tc-8-785-2014>

APPENDIX I

Table 1 - FARO and ATLS specifications

	Wavelength	Measurement Speed	Weight	Range
ATLS	905 nm	2,000 points/second	3.85 kg	500m
FARO	905 nm	976,000 points/second	5.2 kg	0.6-30m

Table 2 - MOSS regression results using distance as a covariate

	10 M	20 M	30 M	40 M
Slope	1.29	1.08	0.75	0.72
Y-Intercept	1.17	3.34	4.75	8.21
r²	0.87	0.71	0.85	0.57
RMSD (cm)	6.55	5.41	2.56	5.50
Mean Difference (cm)	8.47	7.47	4.37	9.61
p-value	0.76	0.42	0.02	0.32

APPENDIX II

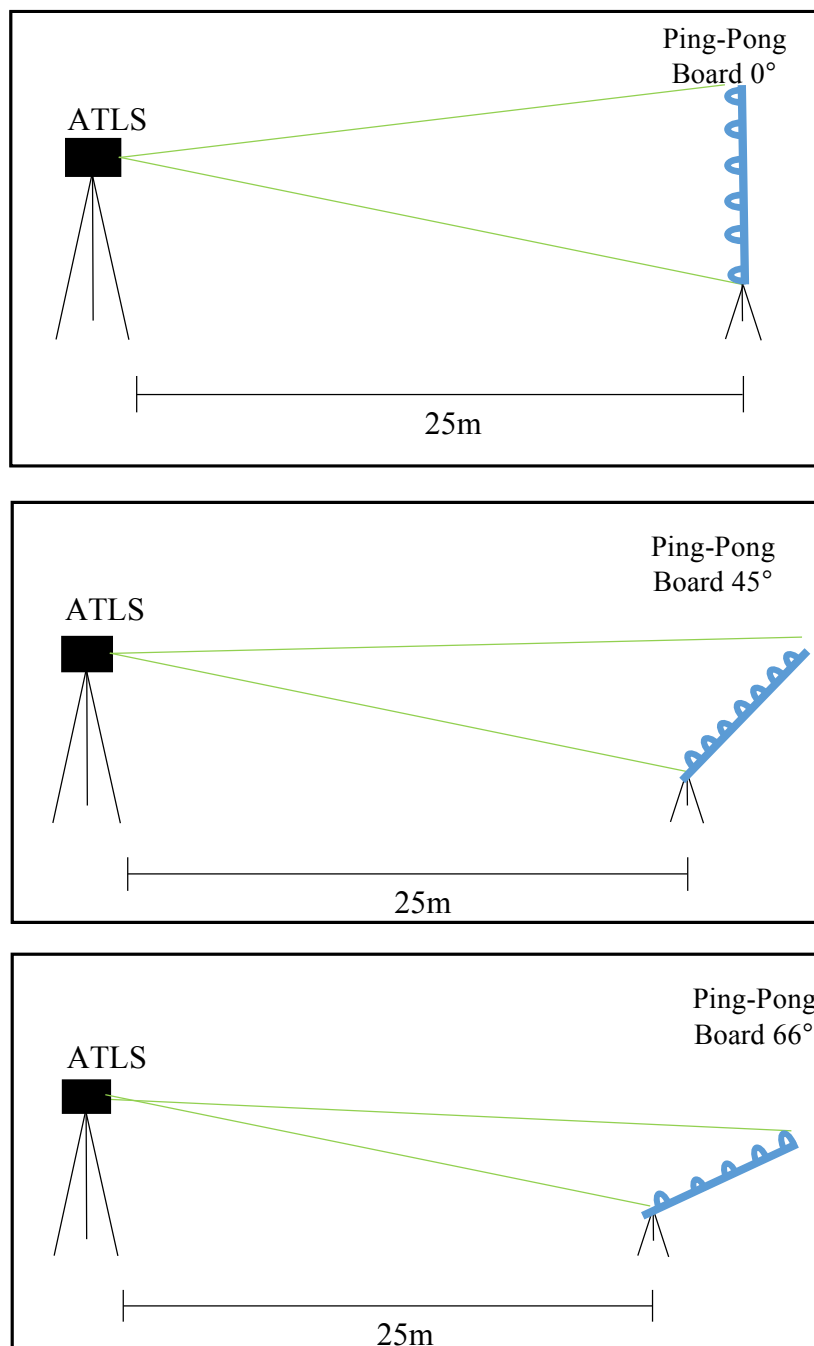


Figure 1 - Diagram of the control study at each angle



Figure 2 - Bear Basin SNOTEL site

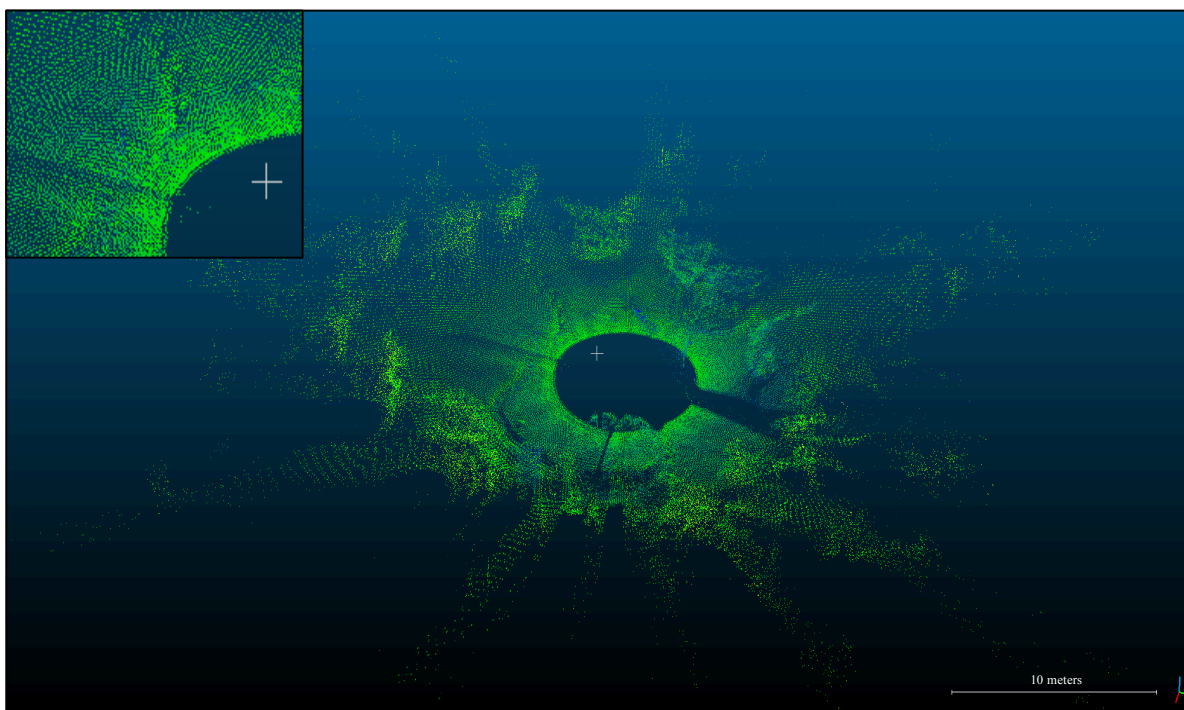


Figure 3 - Bear Basin Cloud Compare 3D Scan including inset to show micro-topography

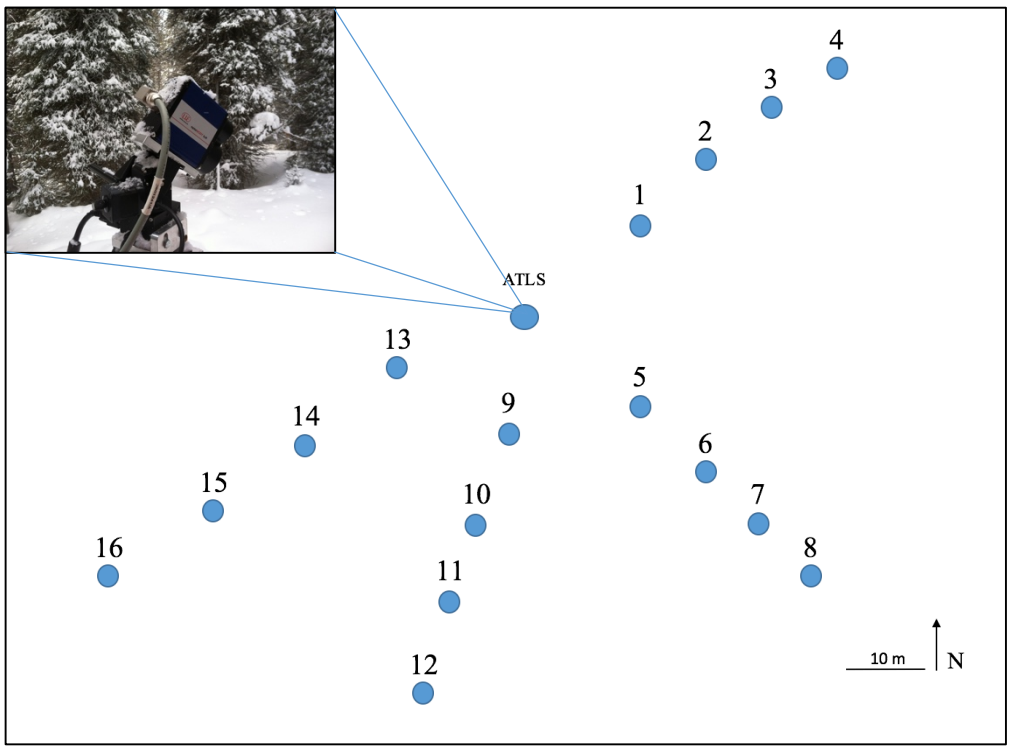


Figure 4 - Diagram of MOSS site

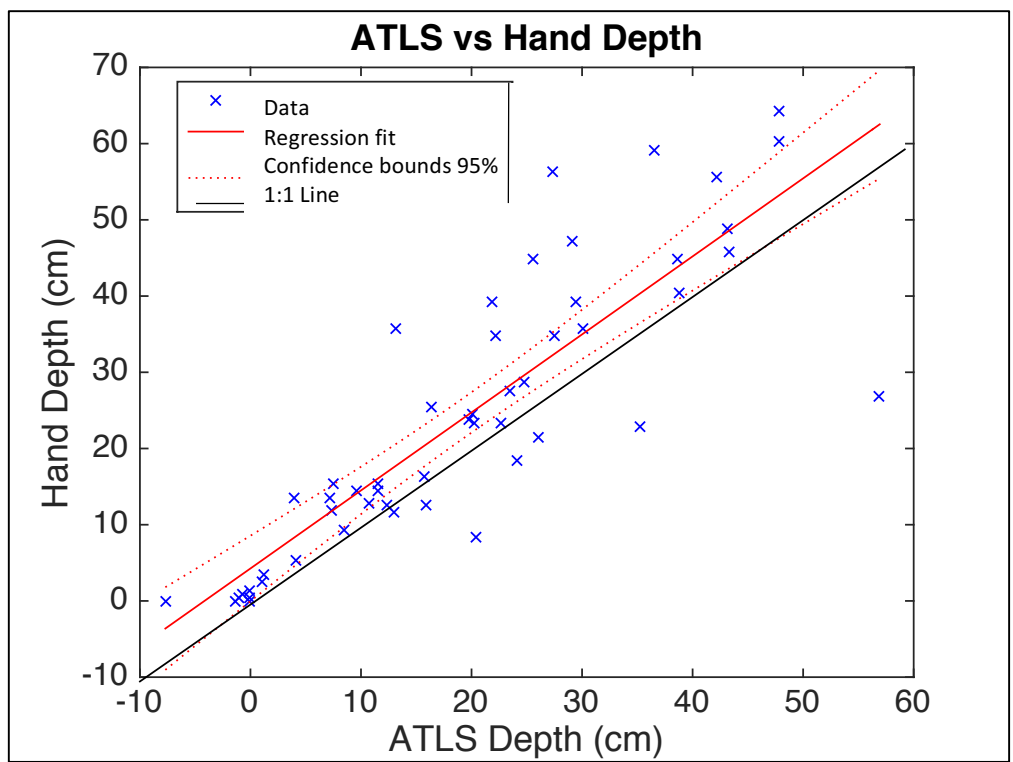


Figure 5 - ATLS and hand depths plotted showing confidence intervals, regression line and 1:1 line

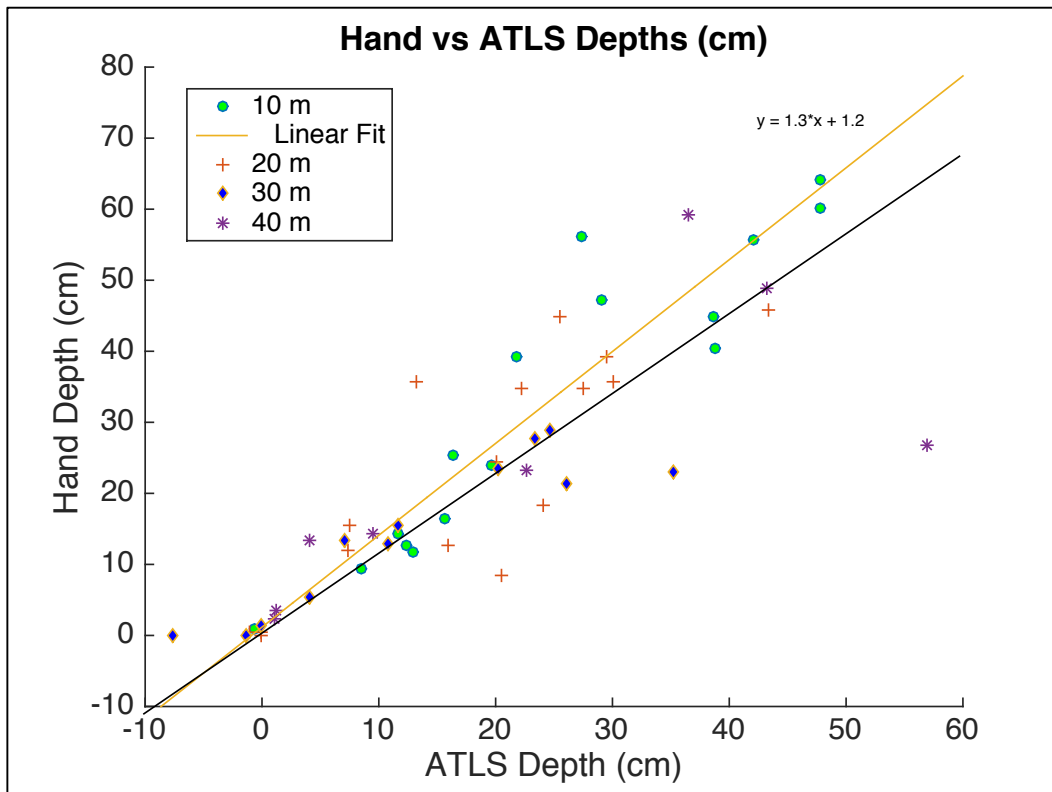


Figure 6 - Hand vs ATLS depths grouped by distance

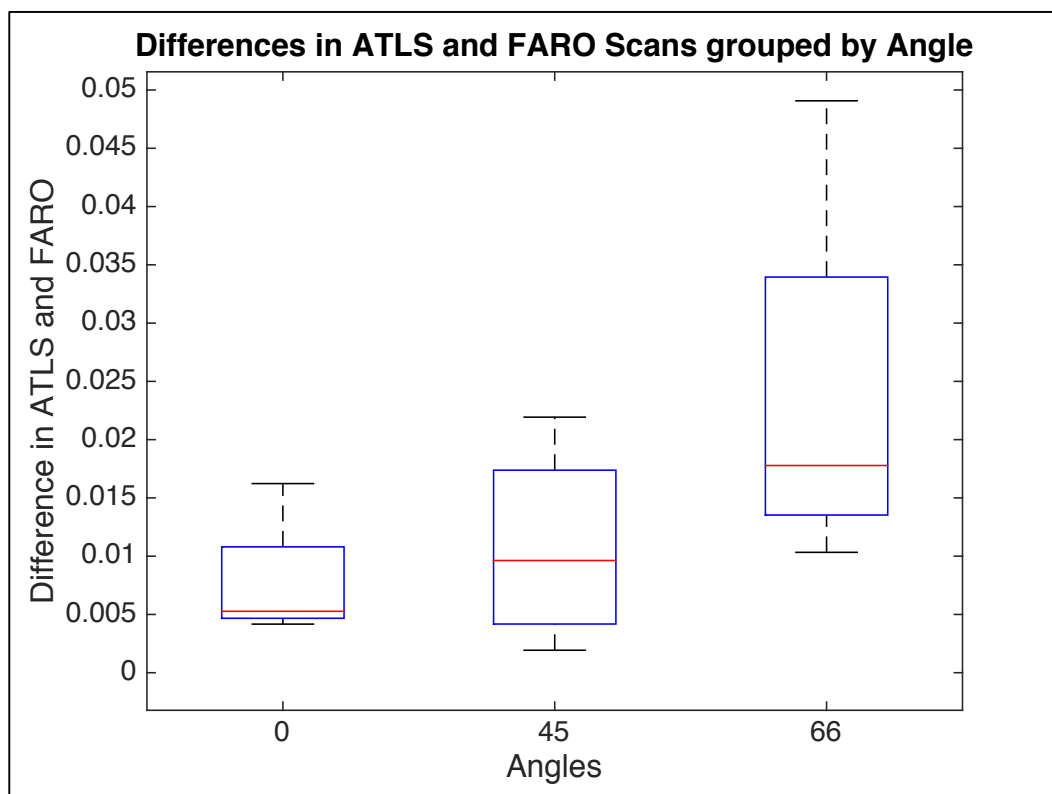


Figure 7 - Boxplot of differences between ATLS and FARO grouped by angles

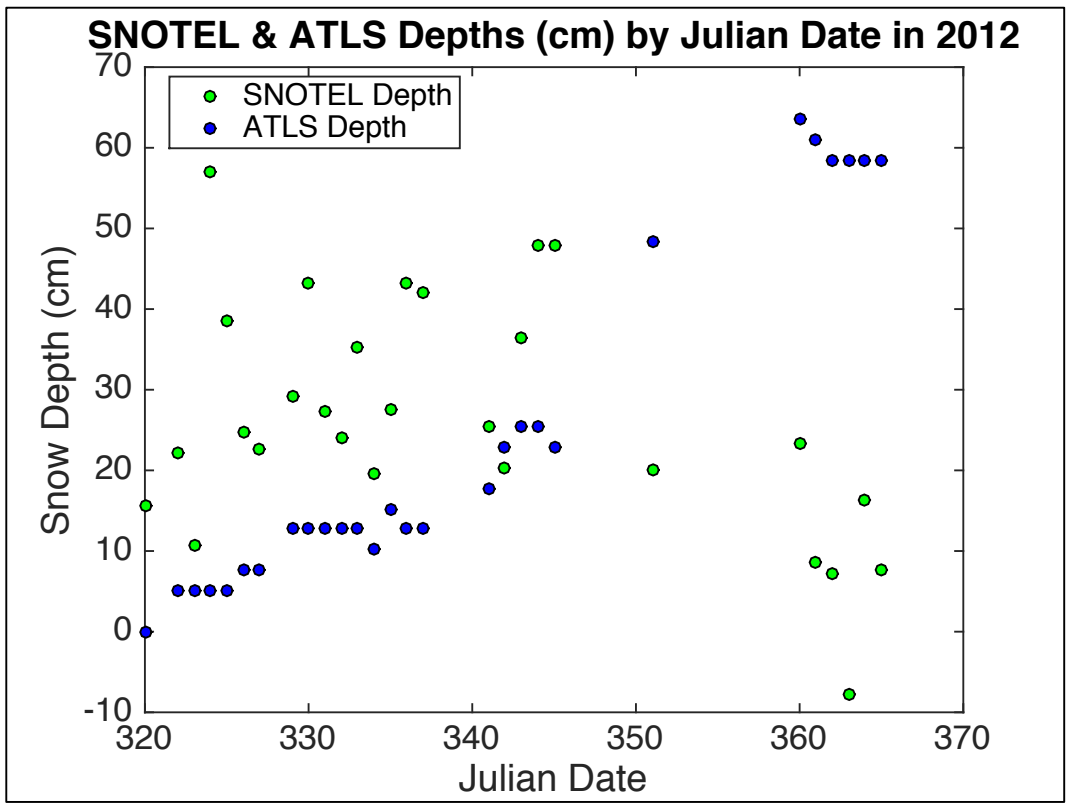


Figure 8 - SNOTEL and ATLS depths plotted by Julian Date in 2012

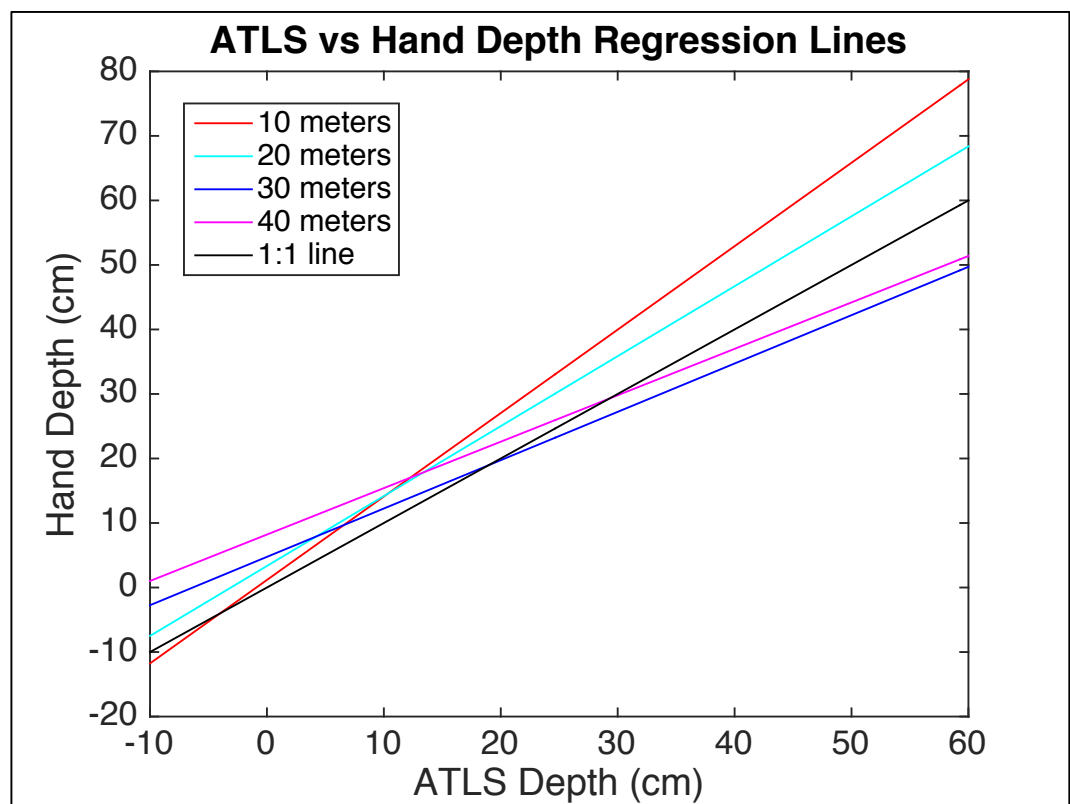


Figure 9 - ATLS and Hand Depth regression lines compared to a 1:1 line

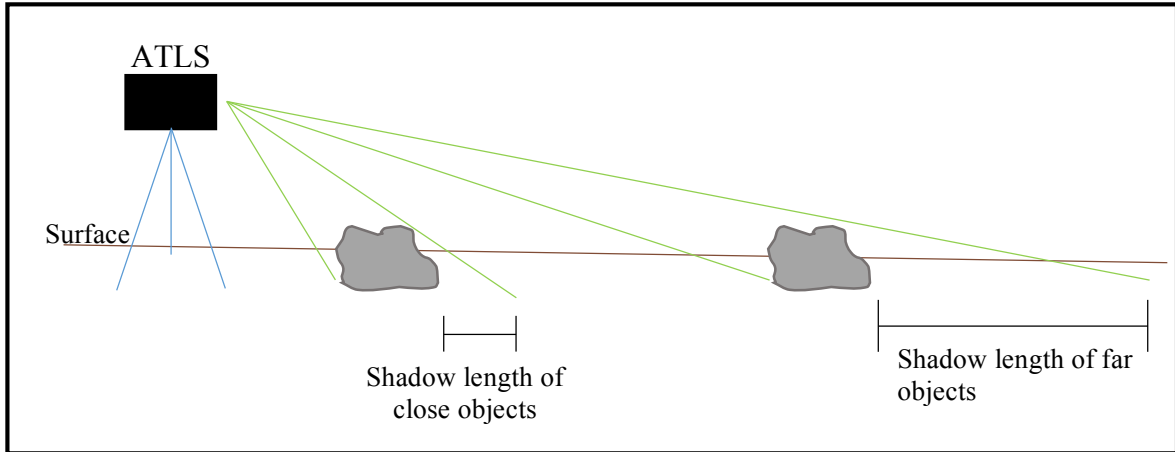
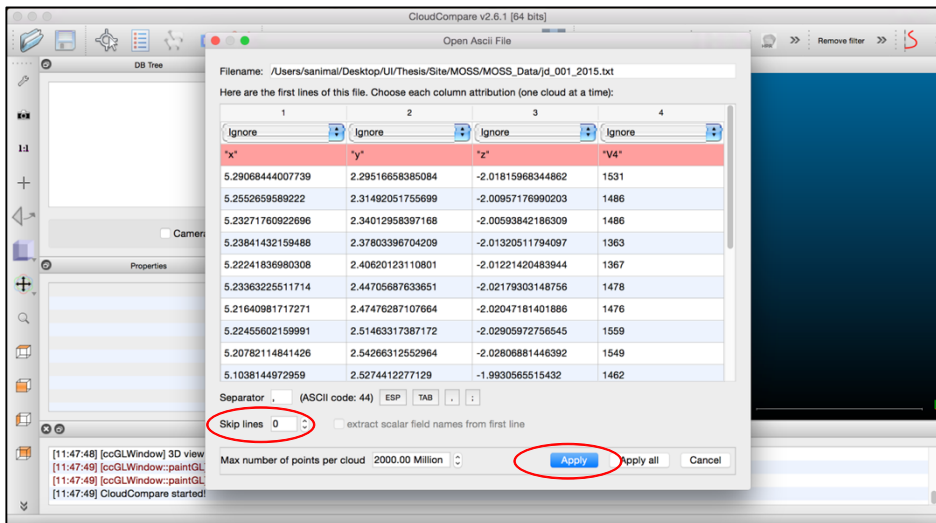


Figure 10 - Shadowing effect

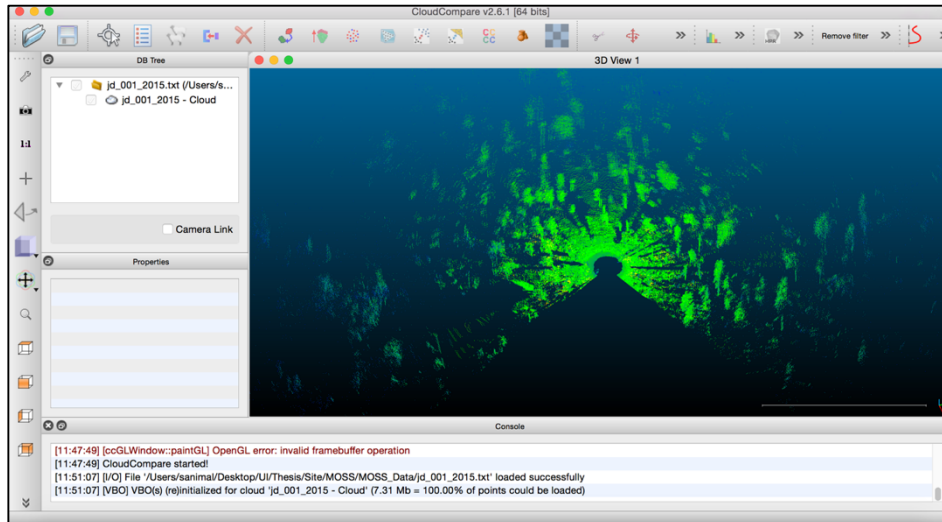
APPENDIX III

This Appendix is a detailed description of the process to load ATLS scans into the free, online software Cloud Compare. The file loaded is an ATLS scan from the MOSS study site taken on January 1, 2015.

1. Open Cloud Compare
2. File > Open > Choose the ATLS data file
3. Skip 1 line if headers are found in data file



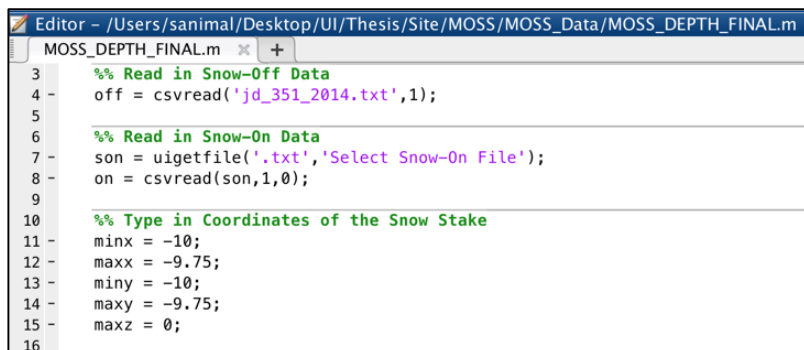
4. Click Apply



APPENDIX IV

This Appendix is a detailed description of the code used to calculate snow depth from ATLS scans using the computer software MATLAB. The files being used are ATLS scans from the MOSS site taken on December 16, 2014 and January 1, 2015, for a snow-free and snow-covered scan, respectively.

1. Open MATLAB
2. Set up correct folder path to the location of ATLS data scans
3. Load snow-free and snow-covered scans
4. Insert coordinates of snow stake (using #9 in the example)

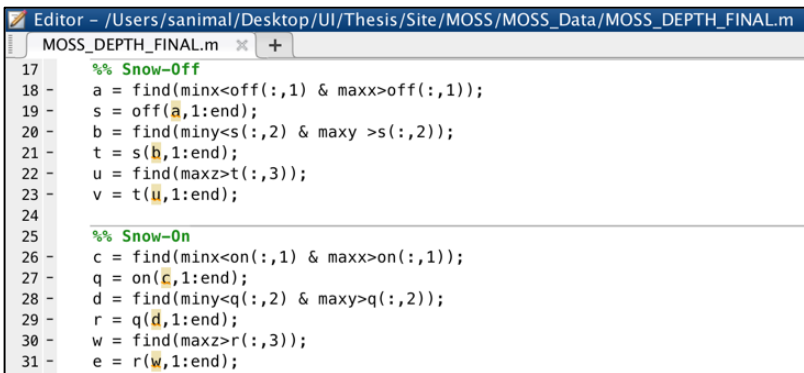


```

Editor - /Users/sanimal/Desktop/UI/Thesis/Site/MOSS/MOSS_Data/MOSS_DEPTH_FINAL.m
MOSS_DEPTH_FINAL.m x +
3   %% Read in Snow-Off Data
4   off = csvread('jd_351_2014.txt',1);
5
6   %% Read in Snow-On Data
7   son = uigetfile('.txt','Select Snow-On File');
8   on = csvread(son,1,0);
9
10  %% Type in Coordinates of the Snow Stake
11  minx = -10;
12  maxx = -9.75;
13  miny = -10;
14  maxy = -9.75;
15  maxz = 0;
16

```

5. Using the find command, eliminate all data other than within the snow stake area

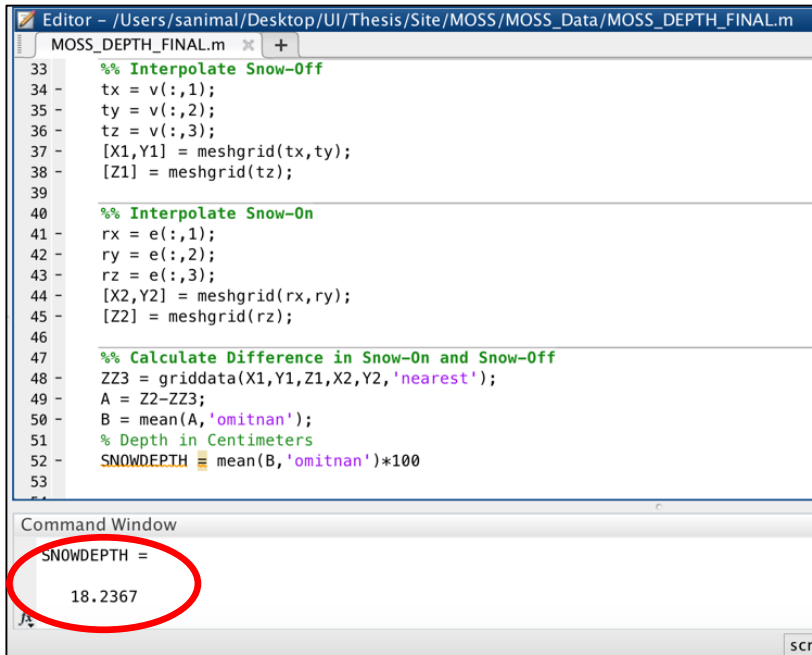


```

Editor - /Users/sanimal/Desktop/UI/Thesis/Site/MOSS/MOSS_Data/MOSS_DEPTH_FINAL.m
MOSS_DEPTH_FINAL.m x +
17  %% Snow-Off
18  a = find(minx<off(:,1) & maxx>off(:,1));
19  s = off(a,1:end);
20  b = find(miny<s(:,2) & maxy >s(:,2));
21  t = s(b,1:end);
22  u = find(maxz>t(:,3));
23  v = t(u,1:end);
24
25  %% Snow-On
26  c = find(minx<on(:,1) & maxx>on(:,1));
27  q = on(c,1:end);
28  d = find(miny<q(:,2) & maxy>q(:,2));
29  r = q(d,1:end);
30  w = find(maxz>r(:,3));
31  e = r(w,1:end);

```

- Interpolate snow-off and snow-on scans, then subtract. The result is the snow depth in centimeters next to snow stake #9 on January 1, 2015.

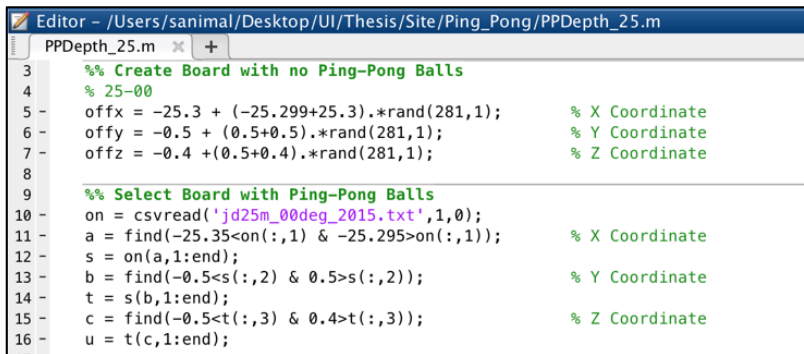


```
Editor - /Users/sanimal/Desktop/UI/Thesis/Site/MOSS/MOSS_Data/MOSS_DEPTH_FINAL.m
MOSS_DEPTH_FINAL.m
33 %% Interpolate Snow-Off
34 tx = v(:,1);
35 ty = v(:,2);
36 tz = v(:,3);
37 [X1,Y1] = meshgrid(tx,ty);
38 [Z1] = meshgrid(tz);
39
40 %% Interpolate Snow-On
41 rx = e(:,1);
42 ry = e(:,2);
43 rz = e(:,3);
44 [X2,Y2] = meshgrid(rx,ry);
45 [Z2] = meshgrid(rz);
46
47 %% Calculate Difference in Snow-On and Snow-Off
48 ZZ3 = griddata(X1,Y1,Z1,X2,Y2,'nearest');
49 A = Z2-ZZ3;
50 B = mean(A,'omitnan');
51 % Depth in Centimeters
52 SNOWDEPTH = mean(B,'omitnan')*100
53
Command Window
SNOWDEPTH =
18.2367
```

APPENDIX V

This Appendix is a detailed description of the code used to calculate ATLS scan differences for the control study using the computer software MATLAB. The example is using the 25 m distance between ATLS and board, and an examples for each 0, 45, and 66° angles are shown.

1. Open MATLAB
2. Set up correct folder path to the location of ATLS data scans
3. Starting with the 0° scan, create a board with no ping pong balls
4. Select the correct ATLS scan and crop to include only the board

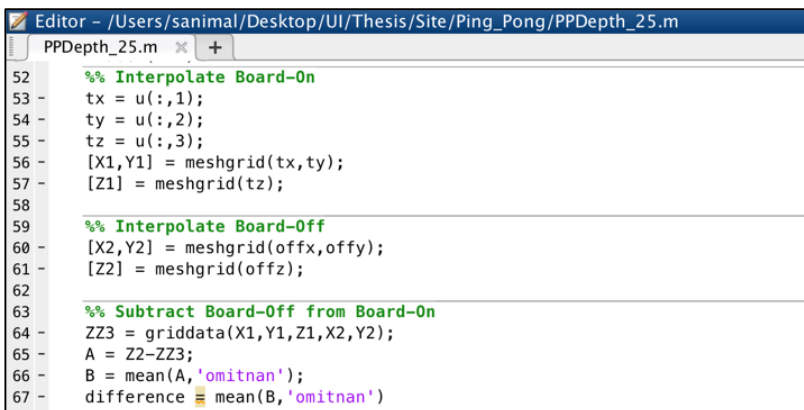


```

Editor - /Users/sanimal/Desktop/UI/Thesis/Site/Ping_Pong/PPDepth_25.m
PPDepth_25.m x +
3   %% Create Board with no Ping-Pong Balls
4   % 25-00
5   offx = -25.3 + (-25.299+25.3).*rand(281,1);      % X Coordinate
6   offy = -0.5 + (0.5+0.5).*rand(281,1);          % Y Coordinate
7   offz = -0.4 + (0.5+0.4).*rand(281,1);          % Z Coordinate
8
9   %% Select Board with Ping-Pong Balls
10  on = csvread('jd25m_00deg_2015.txt',1,0);
11  a = find(-25.35<on(:,1) & -25.295>on(:,1));      % X Coordinate
12  s = on(a,1:end);
13  b = find(-0.5<s(:,2) & 0.5>s(:,2));              % Y Coordinate
14  t = s(b,1:end);
15  c = find(-0.5<t(:,3) & 0.4>t(:,3));              % Z Coordinate
16  u = t(c,1:end);

```

5. Interpolate the board with and board without Ping-Pong balls
6. Subtract Board with and board without, leaving the difference between the two boards



```

Editor - /Users/sanimal/Desktop/UI/Thesis/Site/Ping_Pong/PPDepth_25.m
PPDepth_25.m x +
52  %% Interpolate Board-0n
53  tx = u(:,1);
54  ty = u(:,2);
55  tz = u(:,3);
56  [X1,Y1] = meshgrid(tx,ty);
57  [Z1] = meshgrid(tz);
58
59  %% Interpolate Board-Off
60  [X2,Y2] = meshgrid(offx,offy);
61  [Z2] = meshgrid(offz);
62
63  %% Subtract Board-Off from Board-0n
64  ZZ3 = griddata(X1,Y1,Z1,X2,Y2);
65  A = Z2-ZZ3;
66  B = mean(A,'omitnan');
67  difference = mean(B,'omitnan')

```

7. For the 45° angle, create the board with no Ping-Pong balls in a different way to account for the angle. The values within the equations (i.e. -25.74 and -0.4944) are based on the

location of the point cloud. Use scatter3 to plot the point cloud and determine the location of the corners of the board.

```

Editor - /Users/sanimal/Desktop/UI/Thesis/Site/Ping_Pong/PPDepth_25.m
PPDepth_25.m
18 %% 25-45
19 -   offx = -25.74 + (-25+25.74).*rand(1313,1);
20 -   offy = -0.4944 + (0.5+0.4944).*rand(1313,1);
21 -   offz = offx + 25.4;
22 -   on = csvread('jd25m_45deg_2015.txt',1,0);
23
24 %% Select Board with Ping-Pong Balls
25 -   a = find(-25.74<on(:,1) & -25>on(:,1)); % X Coordinate
26 -   s = on(a,1:end);
27 -   b = find(-0.5<s(:,2) & 0.5>s(:,2)); % Y Coordinate
28 -   t = s(b,1:end);
29 -   c = find(-0.4<t(:,3) & 1>t(:,3)); % Z Coordinate
30 -   u = t(c,1:end);
31

```

8. Follow the previous steps #5-6 to obtain the differences in the boards

9. For the 66° angle, create the board with no Ping-Pong balls in a different way to account for the angle

```

Editor - /Users/sanimal/Desktop/UI/Thesis/Site/Ping_Pong/PPDepth_25.m*
PPDepth_25.m*
32 %% 25-66
33 -   offx = -25.75 + (-25+25.75).*rand(573,1);
34 -   offy = -0.5 + (0.5+0.5).*rand(573,1);
35 -   offz = (-0.42)*offx-10.74;
36 -   off = [offx,offy,offz];
37 -   on = csvread('jd25m_66deg_2015.txt',1,0);
38
39 %% Select Board with Ping-Pong Balls
40 -   oon = [on(:,1),on(:,2),on(:,3)];
41 -   a = find(-25.74<on(:,1) & -25>on(:,1)); % X Coordinate
42 -   s = on(a,1:end);
43 -   b = find(-0.5<s(:,2) & 0.5>s(:,2)); % Y Coordinate
44 -   t = s(b,1:end);
45 -   c = find(-0.25<t(:,3) & 0.1>t(:,3)); % Z Coordinate
46 -   u = t(c,1:end);
47

```

10. Follow the previous steps #5-6 to obtain the differences in the boards

*IF the board was rotated in any other direction than perpendicular (Z-axis) to the board (i.e. Y-axis or X-axis) use the following rotation code (Example from distance 50m and an angle

of 0°)

```

15  %% Create Board with no Ping-Pong Balls
16  % 50-00
17  -  offx = -49.3 + (-49.29+49.3).*rand(506,1);
18  -  offy = -0.15 + (0.8+0.15).*rand(506,1);
19  -  offz = -0.08 +(-1.017+0.08).*rand(506,1);
20
21  %% ROTATE BOARD OFF
22  %% Enter Rotation Point
23  -  v = [offx';offy';offz'];
24  -  x_center = -49.3;
25  -  y_center = -0.1451;
26  -  z_center = -0.6174;
27  -  center = repmat([x_center; y_center; z_center], 1, length(offx));
28  %% Define Angle
29  -  theta = -4; % Degrees
30  -  theta2 = (theta/360)*2*pi; % Converted to Radians
31  %% Rotate
32  -  R = [cos(theta2) -sin(theta2) 0; sin(theta2) cos(theta2) 0; 0 0 1];
33  -  vo = R*(v - center) + center;
34  %% Rotated Values
35  -  xr = vo(1,:)-0.005;
36  -  yr = vo(2,:);
37  -  zr = vo(3,:);
38

```

Use in xr, yr, and zr in place of offx, offy, and offz